# SPIN LABEL STUDY OF ERYTHROCYTE DEFORMABILITY

## $Ca^{2+}$-Induced Loss of Deformability and the Effects of Stomatocytogenic Reagents on the Deformability Loss in Human Erythrocytes in Shear Flow

SUMIHARE NOJI,*‡ SHIGEHIKO TANIGUCHI‡ AND HIDEO KON*
*Laboratory of Chemical Physics, National Institute of Diabetes, and Digestive and Kidney Diseases, National Institutes of Health, Bethesda, Maryland 20892; and ‡Department of Biochemistry, Okayama University Dental School, Shikatacho, Okayama 700, Japan

ABSTRACT The $Ca^{2+}$-induced loss of deformability in human erythrocytes and the recovery of the lost deformability by stomatocytogenic reagents were investigated by means of a new flow electron paramagnetic resonance (EPR) spin label method, which provides information on deformation and orientation characteristics of spin labeled erythrocytes in shear flow. The $Ca^{2+}$-induced loss of deformability is attributed mainly to the increase in intracellular viscosity resulting from efflux of intracellular potassium ions and water (Gardos effect). Partial recovery of the lost deformability is demonstrated in the presence of stomatocytogenic reagents, such as chlorpromazine, trifluoperazine, W-7, and calmidazolium (R24571). The recovery can not be explained solely by suppression of the Gardos effect due to the reagents. Incorporation of an optimal amount of the reagents into the membrane appears to compensate for the membrane modification due to $Ca^{2+}$ ions to restore a part of the lost deformability.

### INTRODUCTION

Human erythrocytes maintain a low concentration of intracellular $Ca^{2+}$ ions at ~0.1–1 $\mu$M by the calcium pump ($Ca^{2+}$-$Mg^{2+}$)-ATPase. When the intracellular $Ca^{2+}$ concentration is increased by a treatment with the calcium ionophore A23187, a series of complex biochemical reactions occurs including the activation of ($Ca^{2+}$-$Mg^{2+}$)-ATPase by $Ca^{2+}$-binding calmodulin (21, 28), the modification of the metabolism and composition of membrane lipids (1–3, 13), and the efflux of $K^+$ ions and water (28, 30) (Gardos effect [16]). It is also known that with an increase in the intracellular $Ca^{2+}$ ion concentration, the cells suffer from a partial loss of the whole cell deformability (11, 20, 22, 26, 40, 43). The erythrocyte deformability is assumed to be generally determined by the following factors: (*a*) physical properties of the membrane and cytoskeleton (e.g., elasticity); (*b*) the state of the cytoplasm (e.g., viscosity, hemoglobin concentration and aggregation); and (*c*) the geometry of the cell (e.g., shape, the surplus of the membrane surface area of the cell relative to its given volume) (14, 19, 23, 32, 35). Of the three factors, the second has been proposed in the past to be the principal mechanism of the $Ca^{2+}$-induced loss of deformability as the result of the cell dehydration and the consequent high internal viscosity (increase in hemoglobin concentration), because no loss of deformability was observed in a high potassium medium in which dehydration and $K^+$ efflux are prevented (11, 20).

Since it was reported recently that some stomatocytogenic calmodulin inhibitors are able to suppress the $Ca^{2+}$-activated $K^+$ efflux in both intact cells and inside-out vesicles (27, 38, 39), it is expected that these reagents may indeed suppress the $Ca^{2+}$-induced deformability loss with concomitant inhibition of the Gardos effect.

In the present work, we used the stomatocytogenic calmodulin inhibitors chlorpromazine (CPZ), trifluoperazine (TFP), W-7 (*N*-[6-aminohexyl]-5-chloro-1-naphthalene sulfonamide), and calmidazolium (CMZ) (R24571, 1-[bis(*p*-chlorophenyl)methyl]-3-[2,4-dichloro-$\beta$-(2,4-dichlorobenzyloxyl)phenethyl]imidazolinium chloride) in an attempt to suppress the $Ca^{2+}$-induced $K^+$ efflux, and examine the effects of such reagents on deformability loss induced by $Ca^{2+}$ loading. To measure the deformability of red blood cells in laminar shear flow, we have utilized the electron paramagnetic resonance (EPR) spin label technique, combined with a computer-regulated variable flow device (23–25, 34, 35). It has been demonstrated experimentally and theoretically that the change in the EPR spectrum of a spin-labeled cell suspension observed in shear flow as compared with that at rest is closely related to the whole cell deformation and orientation (7–9, 23, 34, 35, 37). The method provides a means to assess the degree of deformation and orientation as a function of volume flow rate in intact as well as variously treated cells.

Correspondence should be addressed to Dr. H. Kon, Room B1-14, Building 2, National Institutes of Health, Bethesda, MD 20892.

Our results are consistent with the interpretation that the $Ca^{2+}$-induced deformability loss is mainly due to dehydration of the cells, as has been proposed by Clark et al. (11). Although the stomatocytogenic reagents indeed partially restore the $Ca^{2+}$-induced loss of deformability, the suppression of the Gardos effect by the reagents was found insufficient for complete explanation of the deformability restoration. We propose, therefore, that some other mechanism, such as a recovery of normal membrane elasticity, may also be responsible for the observed partial restoration. It is plausible, for example, that the reagents serve to compensate for the $Ca^{2+}$-induced alteration of the membrane lipid balance to restore a nearly normal mode of bilayer-cytoskeleton interaction.

## MATERIALS AND METHODS

### Preparation of Erythrocyte Suspensions

Fresh heparinized (20 U/ml) human blood, from which buffy coat was removed, was washed three times with an isotonic Hepes buffer (20 mM, pH7.4 adjusted with NaOH) containing 140 mM NaCl and 5 mM KCl. The cells were spin labeled with 5-doxyl stearic acid (Syva Co., Palo Alto, CA) (Fig. 2 *d*) as described before (23). The final concentration of the spin label in the measuring suspension was $3.2 \times 10^{-5}$ M, at which level no morphological changes were observed. The spin-labeled cells were resuspended in the Hepes buffer, which contained 9%(wt/wt) dextran-40 (average molecular weight 40,000) (Sigma Chemical Co., St. Louis, MO) at 35% hematocrit (Ht). The viscosity of the suspending medium was $5.6 \times 10^{-3}$ $Nsm^{-2}$. The final concentration of $Ca^{2+}$ in the measuring suspension was within the range of 20–30 $\mu$M as measured by a calcium electrode (model 93-29; Orion Scientific Instruments Corp., Orion Research Inc., Pleasantville, NY) with an Orion Ionalyzer (model 407). All measurements were completed within 8 h from the start of the preparation.

### Calcium Loading

An appropriate portion of dimethylsufoxide solution (1 mg/ml) of the $Ca^{2+}$ ionophore A23187 (Calbiochem-Behring Corp., American Hoechst, La Jolla, CA) was added to the cell suspension to make up a final concentration between 10 and 20 $\mu$M.

### Calmodulin Inhibitor Agents

Chlorpromazine hydrochloride was purchased from Sigma Chemical Co., calmidazolium (R24571) from Boehringer Mannheim Biochemicals (Indianapolis, IN), W-7 and W-5 from Seikagaku-Kogyo Co. (Tokyo, Japan). Trifluoperazine dihydrochloride and its sulfoxide derivative were the gifts of Smith Kline & French Laboratories (Philadelphia, PA). The drugs were dissolved in dimethylsulfoxide at a concentration of 10–20 mM, and appropriate portions were added to the cell suspension before or after $Ca^{2+}$ loading. Unless otherwise noted, the suspension was incubated at 25°C for 10 min before addition of A23187. For control experiments, the drug solutions were replaced by dimethylsulfoxide.

### Deformability Measurements

The whole cell deformability was measured by the flow-EPR method in a flat quartz EPR cell connected to a syringe drive. The EPR spectral change due to flow was measured at 25°C using a Varian EC-109 X-band spectrometer with 100 KHz magnetic field modulation (modulation amplitude 4 G), equipped with the Laboratory Data Acquisition System built at the NIH Computer Division. The microwave power was kept at 40 mW at which level no power saturation was observed under the present experimental conditions. A computer regulated syringe drive was used to create variable shear stress in the flat EPR cell (wall-to-wall gap 0.27 ± 0.01 mm, length 50 mm, width 8 mm), of which more details were described elsewhere (24). The flat surface of the cell is oriented perpendicularly to the magnetic field. After measuring the peak-to-trough amplitude ($h$) (Fig. 1) in the absence of flow, the magnetic field was held fixed at 3,370 G, at which point the spectral change $\Delta h$ (Fig. 1) due to flow is maximal. The field at which the spectral change is maximal remains the same for a given type of spin label. The normalized spectral change ($\Delta h/h$) was used as an index to assess the degree of cell deformation and orientation in shear flow. The volume flow rate was increased stepwise from 0 to 0.1 ml/s in ~3 min to obtain the spectral change vs. flow rate curve. The volume flow rate of 0.1 ml/s corresponds to the wall shear rate of 1,028 /s. Normally 5 ml of the cell suspension was used.

### Measurements of Hemoglobin Concentration and Packed Cell Volume

The mean cellular hemoglobin concentration (MCHC) was determined from the hematocrit and colorimetric measurement of cyanomethemoglobin (42). The relative change of the packed cellular volume was measured by the capillary centrifuge method.

### Morphological Observations

Cells in suspension at the hematocrit of 35% were fixed in an equal volume of 1% freshly prepared glutaraldehyde solution (Grade I, Sigma Chemical Co., St. Louis, MO) in an isotonic Hepes buffer at room temperature. The photomicrographs were taken using a Nikon Biophot Model VBS microscope (Nihon Kogaku Co., Japan) equipped with differential interference contrast optics. The morphological index was calculated from 100 cell counts on a photograph according to Fujii et al. (15). The positive and negative signs indicate echinocytes and stomatocytes, respectively.

## RESULTS

### Flow-induced Change in EPR Spectra of Spin-labeled Cells

Fig. 1 *a* shows a typical EPR spectrum of the spin-labeled erythrocytes in dextran solution in the absence of flow, when the cells are randomly oriented in the suspension, as illustrated in Fig. 2 *a*. Fatty acid spin labels are known to be incorporated in the membrane with the long axes

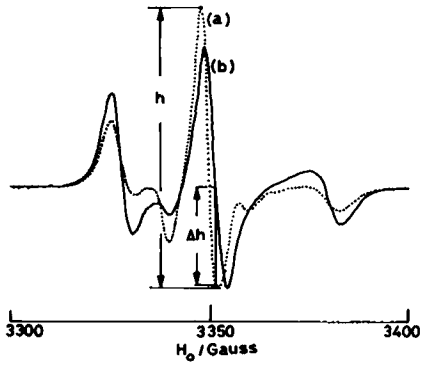


FIGURE 1 EPR spectra of spin labled erythrocytes ($a$) in the absence (·····) and ($b$) presence (——) of flow. Peak-to-trough amplitude ($h$) andthe maximum difference between the two spectra ($\Delta h$) are indicated.

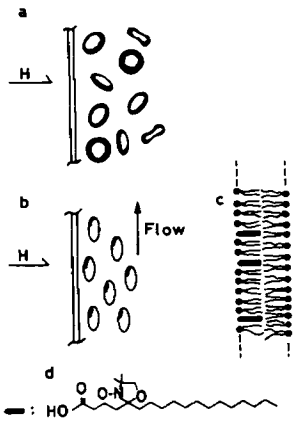


FIGURE 2 Schematic illustrations of (*a*) random orientations of cells at rest, (*b*) orientation and deformation of cells in shear flow, (*c*) incorporation of spin labels into the lipid bilayer, and (*d*) the spin label 5-doxyl stearic acid. *H*, external magnetic field.

aligned approximately perpendicularly to the membrane surface (18) (Fig. 2, *c* and *d*). When the cells are flowing through the flat cell, the red cells elongate and simultaneously orient along the flow direction at various angles due to the flow induced shear stress (23) as shown in Fig. 2 *b*. The combined effect of deformation and orientation causes a change in the spatial distribution of spin labels with respect to the external magnetic field, resulting in a spectral change as shown in Fig. 1 *b*. The increased intensity in the two outer absorptions and the decrease in the center peak indicate that there are more spin labels with their long axes aligned parallel to the external magnetic field direction (or perpendicularly to the flow direction) (Fig. 2, *c* and *d*). Any motion of the cells slower than the time scale of $10^{-5}$ s should not affect the EPR spectral shape (18, 34). Previously, we have demonstrated that the spectral changes are closely correlated with the ability of the cells to deform and orient (23, 34), and the general validity of the model for a flowing red cell was confirmed by computer simulations of the EPR spectra measured at varied flow rates (37). For characterizing the spectral change, the normalized intensity difference $\Delta h/h$ has been used, where $\Delta$ is the maximum spectral change occurring at 3,370 G and $h$ is the amplitude of the center peak in the absence of flow, both in arbitrary units. Thus $\Delta h/h$ may be used for assessing the extent of the average deformation and orientation independently of the signal intensities. In our previous work, the spectral change was characterized by a parameter $l'/l$, the ratio of the amplitudes of the low field and the center absorption (37). That $l'/l$ is linearly related to $\Delta h/h$ can be experimentally demonstrated (data not shown). Further details and applications of the method are described elsewhere (7–9, 23–25, 34, 35, 37). As shown in Fig. 3, the observed parameter $\Delta h/h$ in normal cells generally rises steeply with the flow rate up to ~0.02 ml/s and gradually approaches a plateau around 0.1 ml/s. There is some variance in $\Delta h/h$ vs. flow rate characteristics depending upon the blood specimen, but $\Delta h/h$ values measured in normal cells at 0.1 ml/s generally fall between 0.3 and 0.4. The profile of the individual run is highly reproducible.

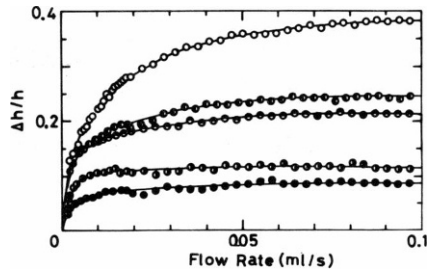


FIGURE 3 Dependence of $\Delta h/h$ on flow rate for $Ca^{2+}$-loaded cells at 0 (○), 8 (◐), 20 (◒), 35 (◑) and 60 (●) min after addition of 10 $\mu$M A23187 in the presence of 20 – 30 $\mu$M $Ca^{2+}$ ion.

## Effect of $Ca^{2+}$-loading on Deformation and Orientation

When the cells are incubated in the presence of $Ca^{2+}$ ions (30 $\mu$M) and $Ca^{2+}$ ionophore A23187, $\Delta h/h$ decreases with time (Figs. 3 and 4). At 35 min after addition of the ionophore, $\Delta h/h$ is down to 0.11 at the flow rate of 0.1 ml/s, indicating that the cells become less deformable and correspondingly less oriented. Few morphological changes are seen in the $Ca^{2+}$-loaded cells before flowing (morphological index +0.04), but most of the cells are converted to the stage I echinocytes (6) (morphological index +1.1) after the flow, probably owing to an enhanced $Ca^{2+}$ ion loading under shear stress (29). In the presence of 1 mM ethylenediamine tetraacetate, the decrease in $\Delta h/h$ did not occur in the cell suspension containing $Ca^{2+}$ ion and the ionophore, demonstrating that $Ca^{2+}$ ions are the agent causing the deformability loss. While the time course of $\Delta h/h$ after $Ca^{2+}$ loading depends somewhat upon the individual blood specimen, a biphasic decrease of $\Delta h/h$ with time is observed as the general trend (Fig. 4). Fig. 4 also shows the simultaneously observed time course for the change in the MCHC after addition of the $Ca^{2+}$ ionophore. The increase in MCHC (or decrease in the cellular volume) is inversely related to the change in $\Delta h/h$, suggesting that the cell dehydration causes the deformability loss. In a high $K^+$ medium (140 mM in place of $Na^+$), neither the decrease in $\Delta h/h$ nor the increase in MCHC is observed in the presence of the $Ca^{2+}$ ionophore. Thus, the loss of the whole cell deformability in $Ca^{2+}$-loaded cells can be explained by the Gardos effect, by which the intracellular viscosity is increased as the result of an

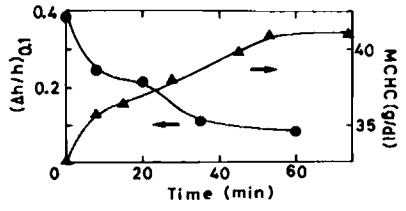


FIGURE 4 The time course of $\Delta h/h$ (●) at the flow rate of 0.1 ml/s and MCHC (▲) after addition of 10 $\mu$M A23187.

enhanced $K^+$ and water extrusion stimulated by the elevated $Ca^{2+}$ level (11). The absence of decrease in $\Delta h/h$ in a high $K^+$ medium also demonstrates that the effect of irreversible membrane protein cross-linking by $Ca^{2+}$ mediated transglutaminase (12), if any, is negligibly small under the present levels of $Ca^{2+}$ loading.

### Effects of Chlorpromazine, Trifluoperazine, and W-7 on $\Delta h/h$ vs. Flow Rate Characteristics in $Ca^{2+}$-loaded Cells

Some calmodulin inhibitors are known to suppress the Gardos effect (27, 38, 39). If the observed loss of the whole cell deformability is due to the Gardos effect, the decrease in $\Delta h/h$ in $Ca^{2+}$-loaded cells is expected to be substantially less in the presence of an inhibitor. We attempt to examine the effects on the cell deformability of four inhibitors, CPZ, TFP, W-7, and CMZ, which are also known to be stomatocytogenic (33). The effect of CMZ, which behaves differently from others, is described separately.

In the presence of 50 $\mu$M CPZ, as shown in Fig. 5, the $\Delta h/h$ vs. flow rate curve, observed at 50 min after adding the $Ca^{2+}$ ionophore, shows an extremely steep rise at the beginning of flow and maintains a higher level than that in the control ($Ca^{2+}$-loaded cells without CPZ) and, even higher than in the intact cells in the low flow rate region below ~0.01 ml/s. No morphological changes were observed photomicrographically before and after the flow in the presence of 50 $\mu$M CPZ (morphological index 0.00). As the flow rate increases, $\Delta h/h$ gradually decreases to the level in the $Ca^{2+}$-loaded cells without CPZ. This may be due to an increase in the intracellular $Ca^{2+}$ concentration during the flow (29), competing against the drug effect.

Since no such enhancement of $\Delta h/h$ is seen in intact cells added with 50 $\mu$M CPZ alone (data not shown), the above described change should be specific to the situation with an elevated cellular $Ca^{2+}$ level. There is also no detectable stomatocyte formation in the present incubation conditions when intact cells are treated with 50 $\mu$M CPZ alone. The recovery peaks at the flow rates 0.01–0.02 ml/s almost independently of the drug concentration. No recovery is observed at 200 $\mu$M CPZ (Fig. 5). The transient recovery of $\Delta h/h$ depends on the CPZ concentration as shown in Fig. 6; the $\Delta h/h$ measured at the flow rate of 0.015 ml/s goes through a maximum at [CPZ] = 50 $\mu$M in $Ca^{2+}$-loaded cells. The morphological index at 100 $\mu$M CPZ before and after the flow was estimated to be −0.09 and 0.00, respectively. The decline of $\Delta h/h$ at higher concentrations may be due to nonspecific drug interactions with the membrane, causing slight morphological changes. The transformation to stomatocytes (morphological index −1) has been reported to occur at 320 $\mu$M in normal cells at Ht 35% (36). The MCHC value at 50 min after addition of $Ca^{2+}$ ionophore remains constant at only a slightly higher level (~41.2 ± 0.05 g/dl) in the presence of CPZ (< 150 $\mu$M), compared with 40.5g/dl without CPZ.

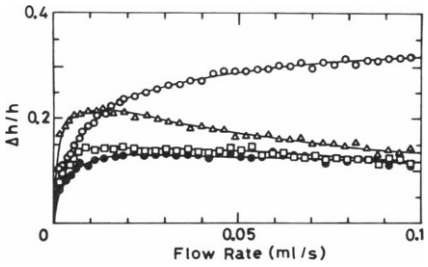


FIGURE 5 Dependence of $\Delta h/h$ on flow rate for intact cells (O), $Ca^{2+}$-loaded cells (□), and $Ca^{2+}$-loaded cells in the presence of 50 $\mu$M (△) and 200 $\mu$M (●) CPZ at 50 min after addition of 20 $\mu$M A23187.

The time courses of $\Delta h/h$ at the flow rate of 0.015 ml/s and of MCHC, for $Ca^{2+}$-loaded cells with and without adding 50 $\mu$M CPZ, are shown in Fig. 7. The loss of deformability due to the elevated $Ca^{2+}$ level is seen to be partly restored by the addition of CPZ; the effect lasts at least over the period of 1.5 h. In the ordinate scales for $\Delta h/h$ and MCHC as shown, the time courses for $\Delta h/h$ and MCHC appear to be inversely related to each other in $Ca^{2+}$-loaded cells without CPZ. On the other hand, the extent of recovery of $\Delta h/h$ due to CPZ in these cells is considerably greater than that which is expected, on the basis of the Gardos effect, from the relatively small differences in MCHC between the systems in the presence and absence of CPZ. The restoration of $\Delta h/h$ was clearly observed even when the difference in MCHC was negligible, for example, at ~1 h after addition of the drug. Thus the observed recovery can not be explained solely by the suppression of the Gardos effect.

Similar results are obtained for TFP and W-7 (Fig. 8), with the maximum recovery dose ranging between 50 and 80 $\mu$M. While the measured MCHC values depend upon the blood specimens (typical values at 30 min after adding the agent at 10 $\mu$M being 43.1 ± 0.4 [41.2 without TFP] and 44.8 ± 0.4 [43.5 without W-7] in grams per decaliter for TFP and W-7, respectively), the individual MCHC in the presence of the drug is found to be independent of the drug concentrations. When a less effective calmodulin antagonist and weaker stomatocytogenic reagent (33), TFP sulfoxide or W-5 (a de-chloro derivative of W-7) is used instead, a smaller deformation recovery is observed (Fig. 8), indicating that the effect of TFP and W-7 in recovery from the $Ca^{2+}$-induced deformability loss is apparently correlated to their calmodulin inhibitory activity or stomatocytogenicity.

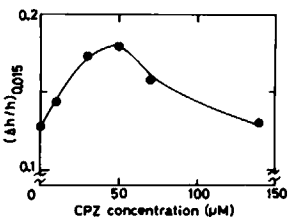


FIGURE 6 Dependence of $\Delta h/h$ at the flow rate of 0.015 ml/s on CPZ concentration for $Ca^{2+}$-loaded cells at 50 min after addition of 20 $\mu$M A23187. The MCHC values for the corresponding CPZ concentration remains constant at 41.2 g/dl.

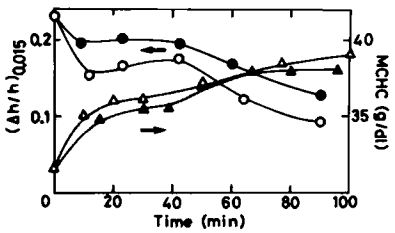


FIGURE 7 The time courses of $\Delta h/h$ (*circles*) at 0.015 ml/s and MCHC (*triangles*) in the absence (*open*) and the presence (*solid*) of 50 $\mu$M CPZ after addition of 10 $\mu$M A23187. A typical result of three repeated experiments.

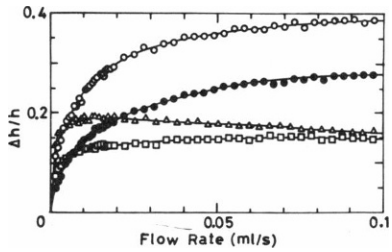


FIGURE 9 Dependence of $\Delta h/h$ on the flow rate for intact cells (O), $Ca^{2+}$-loaded cells (□), and $Ca^{2+}$-loaded cells in the presence of 20 $\mu$M (△) and 75 $\mu$M (●) CMZ at 30 min after addition of 10 $\mu$M A23187.

## Effect of Calmidazolium (CMZ) on $\Delta h/h$ vs. Flow Rate Characteristics in $Ca^{2+}$-loaded Cells

Calmidazolium (R24571) is known as a powerful inhibitor of the calmodulin-dependent fraction of $Ca^{2+}$ transport ATPase (17) and also a potent stomatocytogenic agent (33). The concentration dependence of its effect on $\Delta h/h$-flow rate characteristics is different from that with CPZ, TFP, or W-7, as shown in Fig. 9. Namely, at 20 $\mu$M CMZ, the $\Delta h/h$-flow rate curve shows the sharp rise at the beginning of the flow as in other drugs, but at a higher dose (75 $\mu$M CMZ) the sharp recovery in the low flow rate region vanishes and instead, a marked recovery is observed in the medium to high flow rate region. Thus, $\Delta h/h$ values at 75 $\mu$M CMZ are lower than those at 20 $\mu$M below the flow rate of 0.02 ml/s, above which the 75 $\mu$M dose gives much higher recovery (Fig. 9). The entire feature of the curve at 75 $\mu$M CMZ is similar to that in intact cells. The concentration dependence of $\Delta h/h$ at two flow rates 0.01 and 0.05 ml/s are shown in Fig. 10. The $\Delta h/h$ at 0.01 ml/s reaches a maximum at 20 $\mu$M CMZ, while $\Delta h/h$ at 0.05 ml/s continues to increase at least up to 80 $\mu$M.

Also different from the cases of CPZ, TFP and W-7, the addition of CMZ above 10 $\mu$M causes a decrease in MCHC in $Ca^{2+}$-loaded cells (Fig.10). The increase in $\Delta h/h$ observed at the flow rate of 0.05 ml/s as a function of the drug concentration appears to be inversely related to the corresponding decrease in MCHC (Fig. 10). This is another contrast to the other agents, in which MCHC values were virtually independent of the drug concentrations.

The time courses of $\Delta h/h$ and MCHC at a low flow rate (0.015 ml/s) after addition of CMZ to $Ca^{2+}$-loaded cells are shown in Fig. 11. In the absence of CMZ, there is a sharp decline in $\Delta h/h$ during the first 10 min with corresponding increase in MCHC, reflecting the elevated $Ca^{2+}$ level. In the presence of CMZ, an appreciable recovery in $\Delta h/h$ appears over the time course of 1 h, and concomitantly the MCHC stays consistently lower than in the control, indicating a partial suppression of the Gardos effect. Thus, the observed restoration of $\Delta h/h$ by CMZ may be attributed at least partly to the reduced level of the Gardos effect. However, the other mechanism for restoration such as the one expressed in the other agents may be operating simultaneously, since the effect of CMZ on $\Delta h/h$ is not in proportion to that on MCHC (Fig. 11).

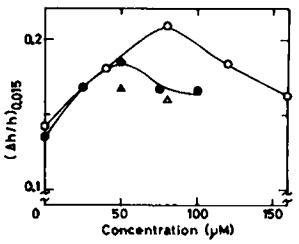


FIGURE 8 Dependence of $\Delta h/h$ at the flow rate of 0.015 ml/s on (*a*) TFP (O) (TFP sulfoxide [△]) and (*b*) W-7 (●) (W-5 [▲]) concentrations in $Ca^{2+}$-loaded cells. The MCHC values for the corresponding concentrations remain constant at 43.1 and 44.8 g/dl for TFP and W-7, respectively.

## DISCUSSION

We have reconfirmed by the flow-EPR spin-label method the loss of the whole cell deformability in $Ca^{2+}$-loaded erythrocytes. The observations in which the time courses of $\Delta h/h$ and MCHC are inversely correlated even to the point of mimicking the biphasic profiles in each other (Figs. 7 and 11) and that such changes are completely suppressed when the cells are suspended in a high $K^+$ medium, provide a sufficient basis for concluding that the deformability loss is the result of $Ca^{2+}$-activated $K^+$ and water extrusion and of the consequent increase in intracellular viscosity, as was proposed by Clark et al. (11).

Since it has been demonstrated that the presence of calmodulin causes a $Ca^{2+}$-dependent increase in the $K^+$ permeability (30, 38) and the calmodulin antagonists at a proper dose level block the $K^+$ extrusion (27, 39), the loss of deformability in $Ca^{2+}$-loaded cells is expected to be restored to some extent by adding a calmodulin inhibitor. In fact, appreciable restoration of $\Delta h/h$ is seen in the

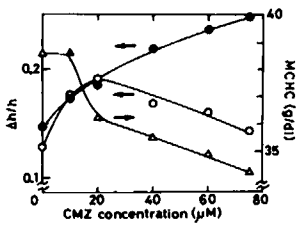


FIGURE 10 Dependence of $\Delta h/h$ at 0.01 (O) and 0.05 (●) ml/s, and MCHC (△) on CMZ concentrations at 30 min after addition of 10 $\mu$M A23187.

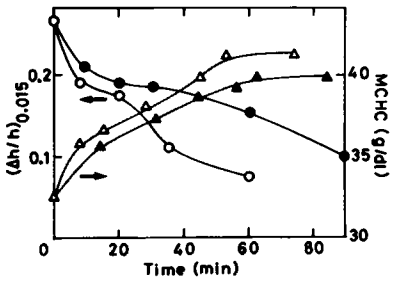


FIGURE 11 The time courses of $\Delta h/h$ (*circles*) at the flow rate of 0.015 ml/s and MCHC (*triangles*) for $Ca^{2+}$-loaded cells in the absence (*open*) and presence (*solid*) of 20 $\mu$M CMZ.

presence of all the inhibitors tested, even though the Gardos effect is never completely suppressed. Clear evidence for the effect of the agent on cellular volume (or MCHC) is obtained only with CMZ (Fig. 10), especially at a high dose level. When the restoration of deformability is the result of a partial suppression of $H_2O$ efflux (i.e., a less viscous cytosol), $\Delta h/h$ should be evenly elevated over the entire range of the flow rate as indeed is the case with CMZ (Fig. 9). In the remaining reagents, CPZ, TFP, and W-7, the effect on the cell volume in $Ca^{2+}$-loaded cells is only marginal, indicating that the Gardos effect is almost fully activated at the selected dose levels. Nevertheless, the deformability of $Ca^{2+}$-loaded cells is substantially restored by the reagents, suggesting that some mechanism other than the suppression of the Gardos effect may be operating in the recovery. The dose rate per cell, e.g., of CPZ used in the present work is estimated to be ~1/30 of that used by other workers (27) to suppress > 90% of $K^+$ extrusion activity. Raising the dose level further in the present experiments resulted in a lesser deformability restoration, probably due to the onset of stomatocytosis (31, 33) and other nonspecific disturbances. Thus, there seems to be an optimal dose level for observing the restoration.

Except for the case of CMZ at a high dose level, restorations are normally evident in the low shear rate regions. This may be interpreted to indicate a change in membrane properties, such as a lower modulus of elasticity influencing the whole cell deformability. In the opposite cases of a hardened membrane, either by cross-linking or heat denaturation of spectrin, the reduction of $\Delta h/h$ was especially marked in the low to medium shear rate region, and $\Delta h/h$ gradually approaches the control level at high shear rates (23, 32).

There have been suggestions concerning the membrane deformability modifications associated with a low level $Ca^{2+}$ loading, but no clear evidence has so far been presented. In a study by the ektacytometry (11), the immediate effect of a low level $Ca^{2+}$ loading on the membrane property could not be clearly demonstrated because of the combined effect of increased internal viscosity and the decreased surface-to-volume ratio, but a slight reduction in the initial slope of deformation index was reported in some cases in high $K^+$ media at high $Ca^{2+}$ concentrations > 500 $\mu$M. Similarly, in $Ca^{2+}$-treated resealed ghosts, the reduction of the membrane deformability was demonstrated only at concentrations much higher than 100 $\mu$M (20). The proper use of stomatocytogenic agents in the present work raised a strong possibility that part of the deformability loss by $Ca^{2+}$ ions may be caused by some membrane property change that is masked by the Gardos effect in $Ca^{2+}$ loading alone.

A plausible explanation for the recovery effect, except for the part in which suppression of the Gardos effect is clearly responsible, may be based upon the activity of the reagents as stomatocyte formers or as calmodulin inhibitors. An enhanced intracellular $Ca^{2+}$ concentration, even at a relatively low level, is known to induce a complex variety of biochemical events involving several membrane lipids and proteins (3). A relevant process in the present context may be the breakdown of polyphosphoinositides, which was shown to cause profound changes in the membrane balance and has been implicated in the process of echinocytosis (1, 4, 13). That incorporation of an echinocytogenic reagent into the membrane has an effect on the rheological properties of the cell, especially in the low shear characteristics, has been demonstrated (31). The deformability of an erythrocyte may be related to the balance of the lipid bilayer through a close coupling between the lipid bilayer and the cytoskeletal proteins (4, 19). In the absence of the stomatocytogenic reagents, and at the $Ca^{2+}$ ion concentrations used in the present work, echinocytosis is latent before flow but becomes visible after flow. In the presence of a stomatocytogenic reagent at an optimal dose level, intercalation of the reagent into the membrane inner layer is likely to compensate for the imbalance and restore a near normal physical state, even though no explicit morphological changes were observed.

If, on the other hand, it can be established that the reagents used actually act as calmodulin inhibitors within the cell, a possible explanation may be sought along the line of the $Ca^{2+}$-dependent binding of calmodulin to spectrin (5, 10, 21, 41), which may modify the visco-elastic properties of the cytoskeleton. Regulation of the cell morphology through $Ca^{2+}$ ion-activated calmodulin, however, appears to be unlikely, since it has been shown that CPZ causes stomatocytosis even in $Ca^{2+}$-depleted erythrocytes (10).

*Received for publication 9 January 1987.*

## REFERENCES

1. Allan, D., and R. H. Michell. 1978. A calcium-activated polyphosphoinositide phosphodiesterase in the plasma membrane of human and rabbit erythrocytes. *Biochim. Biophys. Acta.* 508:277–286.
2. Allan, D., and P. Thomas. 1981. $Ca^{2+}$-induced biochemical changes in human erythrocytes and their relation tomicro-vesiculation. *Biochem. J.* 198:433–440.
3. Allan, D., and P. Thomas. 1981. The effects of $Ca^{2+}$ and $Sr^{2+}$ on

$Ca^{2+}$-sensitive biochemical changes in human erythrocytes and their membranes. *Biochem. J.* 198:441–445.

4. Anderson, R. A., and V. T. Marchesi. 1985. Regulation of the association of membrane skeletal protein 4.1 with glycophorin by a polyphosphoinositide. *Nature (Lond.).* 318:259–298.
5. Berglund, A., L. Backman, and V. P. Shanbhag. 1984. Calmodulin binding to human spectrin. *FEBS (Fed. Eur. Biochem. Soc.) Lett.* 172:109–113.
6. Bessis, M. 1973. Red cell shapes: an illustrated classification and its rationale. *In* Red Cell Shape. M. Bessis, R. I. Weed, and P.F. Leblond, editors. Springer-Verlag, New York. 1–25.
7. Bitbol, M., and F. Leterrier. 1982. Measurement of the erythrocyte orientation in a flow by spin labeling. I. Comparison between experimental and numerically simulated E.P.R. spectra. *Biorheology.* 19:669–680.
8. Bitbol, M., and D. Quemada. 1985. Measurement of erythrocyte orientation in flow by spin labeling. II. Phenomenological models for erythrocyte orientation rate. *Biorheology.* 22:31–41.
9. Bitbol, M., F. Leterrier, J. Dufaux, and D. Quemada. 1985. Measurement of erythrocyte orientation in flow by spin labeling. III. Erythrocyte orientation and rheological conditions. *Biorheology.* 22:43–53.
10. Burns, N. R., and W. B. Gratzer. 1985. Interaction of calmodulin with the red cell and its membrane skeleton and with spectrin. *Biochemistry.* 24:3070–3074.
11. Clark, M. R., N. Mohandas, C. Feo, M. S. Jacobs, and S. B. Shohet. 1981. Separate mechanisms of deformability loss in ATP-depleted and Ca-loaded erythrocytes. *J. Clin. Invest.* 67:531–539.
12. Coetzer, T. L., and S. S. Zail. 1979. Cross-linking of membrane proteins of metabolically-depleted and calcium-loaded erythrocytes. *Br. J. Haematol.* 43:375–390.
13. Ferrell, J. E., Jr., and W. H. Huestis. 1984. Phosphoinositide metabolism and the morphology of human erythrocytes. *J. Cell. Biol.* 98:1992–1998.
14. Fischer, T. M., C. W. M. Haest, M. Stöhr, D. Kamp, and B. Deuticke. 1978. Selective alteration of erythrocyte deformability by SH-reagents. Evidence for an involvement of spectrin in membrane shear elasticity. *Biochim. Biophys. Acta.* 510:270–282.
15. Fujii, T., T. Sato, A. Tamura, M. Wakatsuki, and Y. Kanaho. 1979. Shape changes of human erythrocytes induced by various amphipathic drugs acting on the membrane of the intact cells. *Biochem. Pharmacol.* 28:613–620.
16. Gardos, G. 1966. The mechanism of ion transport in human erythrocytes. *Acta Biochim. Biophys. Acad. Sci. Hung.* 1:139–148.
17. Gietzen, K., A. Wuthrich, and H. Bader. 1981. R24571: a new powerful inhibitor of red blood cell $Ca^{2+}$-transport ATPase and of calmodulin-regulated functions. *Biochem. Biophys. Res. Commun.* 101:418–425.
18. Griffith, O. H., and P. C. Jost. 1976. Lipid spin labels in biological membranes. *In* Spin Labeling. Vol. 1. L. J. Berliner, editor. Academic Press, Inc., New York. 454–519.
19. Haest, C. W. M. 1982. Interactions between membrane skeleton proteins and the intrinsic domain of the erythrocyte membrane. *Biochim. Biophys. Acta.* 694:331–352.
20. Heath, B. P., N. Mohandas, J. L. Wyatt, and S. B. Shohet. 1982. Deformability of isolated red blood cell membranes. *Biochim. Biophys. Acta.* 691:211–219.
21. Husain, A., G. J. Howlett, and W. H. Sawyer. 1984. The interaction of calmodulin with human and avian spectrin. *Biochem. Biophys. Res. Commun.* 122:1194–1200.
22. Kirkpatrick, F. H., D. G. Hillman, and P. L. LaCelle. 1975. A23187 and red cells: changes in deformability, $K^+$, $Mg^{2+}$, $Ca^{2+}$ and ATP. *Experientia (Basel).* 31:653–654.
23. Kon, K., S. Noji, and H. Kon. 1983. Spin label study of erythrocyte deformability. III. Further characterizations of electron spin resonance spectral change in shear flow. *Blood Cells (Berl.).* 9:427–438.
24. Kon, K., E. R. O'Bryan, and H. Kon. 1985. Effect of the presence of hardened erythrocytes on deformation-orientation characteristics of normal erythrocytes in shear flow studied by the spin label method. *Biorheology.* 22:105–117.
25. Kon, K., and H. Kon. 1985. Study of the effect of varying hematocrit on free deformation and orientation of erythrocytes in flow. *Biorheology.* 22:323–333.
26. Kuettner, J. F., K. L. Dreher, G. H. R. Rao, J. W. Eaton, P. L. Blackshear, Jr., and J. G. White. 1977. Influence of the ionophore A23187 on the plastic behavior of normal erythrocytes. *Am. J. Pathol.* 88:81–94.
27. Lackington, I., and F. Orrego. 1981. Inhibition of calcium-activated potassium conductance of human erythrocytes by calmodulin inhibitory drugs. *FEBS (Fed. Eur. Biochem. Soc.) Lett.* 133:103–106.
28. Lake, W., H. Rasmussen, and D. B. P. Goodman. 1977. Effect of ionophore A23187 upon membrane function and ion movement in human and toad erythrocytes. *J. Membr. Biol.* 32:93–113.
29. Larsen, F. L., S. Katz, B. D. Roufogalis, and D. E. Brooks. 1981. Physiological shear stresses enhance the $Ca^{2+}$ permeability of human erythrocytes. *Nature (Lond.).* 294:667–668.
30. Lassen, U. V., L. Pape, and B. Vestergaard-Bogind. 1980. Calcium related transient changes in membrane potential of red cells. *In* Membrane Transport in Erythrocytes. Alfred Benzon Symposium. Vol. 14. U.V. Lassen, H. H. Ussing, and J. O. Wieth, editors. Munksgaard, Copenhagen. 255–273.
31. Meiselman, H. J. 1981. Morphological determinants of red cell deformability. *Scand. J. Clin. Lab. Invest.* 41:(Suppl.156):27–34.
32. Mohandas, N., M. R. Clark, M. S. Jacobs, and S. B. Shohet. 1980. Analysis of factors regulating erythrocyte deformability. *J. Clin. Invest.* 66:563–573.
33. Nelson, G. A., M. L. Andrews, and M. J. Karnovsky. 1983. Control of erythrocyte shape by calmodulin. *J. Cell. Biol.* 96:730–735
34. Noji, S., F. Inoue, and H. Kon. 1981. Spin label study of erythrocyte deformability. I. Electron spin resonance spectral change under shear flow. *Blood Cells (Berl.).* 7:401–411.
35. Noji, S., F. Inoue, and H. Kon. 1981. Use of spin label and the flow -induced ESR spectral difference for studying erythrocyte deformation. *J. Biochem. Biophys. Methods.* 5:251–258.
36. Noji, S., T. Takahashi, and H. Kon. 1982. A spin-label study of the correlation between stomatocyte formation and membrane fluidization of erythrocytes. *Biochem. Pharmacol.* 31:3173–3180.
37. Noji, S., H. Kon, and S. Taniguchi. 1984. Spin label study of erythrocyte deformability. IV. Relation of ESR spectral change with deformation and orientation of erythrocytes in shear flow. *Biophys. J.* 46:349–355.
38. Pape, L., and B. I. Kristensen. 1984. A calmodulin activated $Ca^{2+}$ -dependent $K^+$ channel in human erythrocyte membrane inside-out vesicles. *Biochim. Biophys. Acta.* 770:1–6.
39. Sanchez, A., J. Garcia-Sancho, and B. Herreros. 1980. Effects of several inhibitors on the $K^+$ efflux induced by activation of the $Ca^{2+}$ -dependent channel and by valinomycin in the human red cell. *FEBS (Fed. Eur. Biochem. Soc.) Lett.* 110:65–68.
40. Shiga, T., M. Sekiya, N. Maeda, K. Kon, and M. Okazaki. 1985. Cell age-dependent changes in deformability and calcium accumulation of human erythrocytes. *Biochim. Biophys. Acta.* 814:289–299.
41. Sobue, K., Y. Muramoto, M. Fujita, and S. Kakiuchi. 1981. Calmodulin-binding proteins of erythrocyte cytoskeleton. *Biochem. Biophys. Res. Commun.*100:1063–1070.
42. Von Kampen, E. J., and W. G. Zijlstra. 1961. Standardization of hemoglobinometry. II. The hemiglobincyanide method. *Clin. Chim. Acta.*6:538–544.
43. Weed., R. I., P. L. LaCelle, and E. W. Merrill. 1969. Metabolic dependence of red cell deformability. *J. Clin. Invest.* 48:795–809.